Short-range order in liquid Na - Cd alloys

1996 J. Phys.: Condens. Matter 8 8105

(http://iopscience.iop.org/0953-8984/8/43/008)

J. Phys.: Condens. Matter **8** (1996) 8105–8119. Printed in the UK

Short-range order in liquid Na–Cd alloys

Z H Jin, K Y Chen, K Lu and Z Q Hu

State Key Laboratory of RSA, Institute of Metal Research, Academia Sinica, Shenyang, 110015, People's Republic of China

Received 12 March 1996, in final form 15 May 1996

Abstract. We present a detailed study of both the topological and the chemical short-range orders for liquid Na–Cd alloys using interatomic potentials derived from a non-local model pseudopotential theory. First, the mixing entropy is predicted using a hard-sphere Yukawa reference system, with the parameters being measured from the pseudopotential-calculated mean interatomic interactions and the ordering potentials. It is found that the ordering contribution to the entropy reaches its largest magnitude at around 30 to 50 at.% (atomic per cent) of Na, while above 70 at.% Na, the contribution is small. Then, the atomic structures are calculated using molecular dynamics simulations combined with an energy mapping technique. From the careful examination of the calculated structural distribution functions, the chemical short-range-order parameters and the pair analysis results, we found that with increasing Na concentration, the Na–Cd alloy system exhibits a chemical ordering tendency from compound forming to phase separation, and a topological ordering tendency from a Cd-like structure characterized by 1311- and 1422-type atomic bonded pairs to a Na-like one characterized by 1551-type atomic bonded pairs.

1. Introduction

The liquid Na–Cd alloy system exhibits quite interesting thermodynamic properties. A careful examination of the entropy of alloy formation (Tamaki and Cusack 1979, Hoshino and Endo 1982, Iwase *et al* 1985, Harada *et al* 1988) ΔS leads to the following three points. First, ΔS deviates negatively from that of the ideal mixture. This suggests that there is a considerable volume contraction for this system. In fact, Hoshino and Endo (1982) found volume contraction as large as 14% for the equiatomic NaCd alloy. Second, ΔS deviates very considerably from the ideal mixing entropy at low concentrations of Na. This indicates a compound-forming (CF) tendency of the Cd-rich liquid alloys. And third, ΔS reaches its maximum above the concentration of 70 at.% Na, so a tendency towards phase separation (PS) may be expected for the Na-rich alloys. Since alloys with chemical interactions are always characterized by volume contractions (see, e.g., Ruppersberg and Speicher 1976), the above first and the second points can be attributed to the same chemical origin. It has been verified by Karaoglu and Young (1990) that, in using a non-rigid-core hard-sphere model, the excess entropy can be successfully reproduced. They argued that the CF tendency is generally weak in the Na–Cd alloy as compared with other cases such as Na–Ga, Na–Sn and Li–Pb. Since all of these remarks are drawn from the thermodynamic point of view, further insight as regards both the topological short-range order (TSRO) and the chemical short-range order (CSRO) for Na–Cd alloys is still needed. And this is our main goal in this paper.

0953-8984/96/438105+15$19.50

The interatomic potentials are calculated using the energy-independent non-local model pseudopotential (EINMP) theory in a theoretical study of both TSRO and CSRO for liquid Na–Cd metallic alloys. The EINMP has been used by Wang and Lai (1980) and co-workers (Li *et al* 1986) in the investigation of the thermodynamics, structures and electron transport properties for simple alloys. The crucial point is that, unlike in the former work of Wang, Lai *et al*, we use the Ichimaru and Utsumi (1981) type of exchange–correlation function in the description of the screening of the pseudopotentials. Thus-calculated interatomic potentials have been proved to be more reliable, not only for pure metals such as Ga (Tsay and Wang 1994) and Cd, but also for binary alloys such as some Li-based binary alloys (Li–In, Li–Ga or Li–Tl) and the case studied here, Na–Cd. Detailed remarks on this aspect are presented in section 2.

The rest of this paper is organized as follows. In section 3, we show that making a meaningful prediction of the excess entropy of Na–Cd is possible by using a hard-sphere Yukawa (HSY) model, with the parameters being measured from the effective interatomic potentials. In section 4, the liquid structures are simulated using molecular dynamics (MD) techniques combined with a potential energy mapping method proposed by Stillinger and Weber (1982). We focus our attention on a careful examination of the structural features for Na–Cd over the whole concentration range both before and after the energy mappings. Conclusions are finally drawn in section 5.

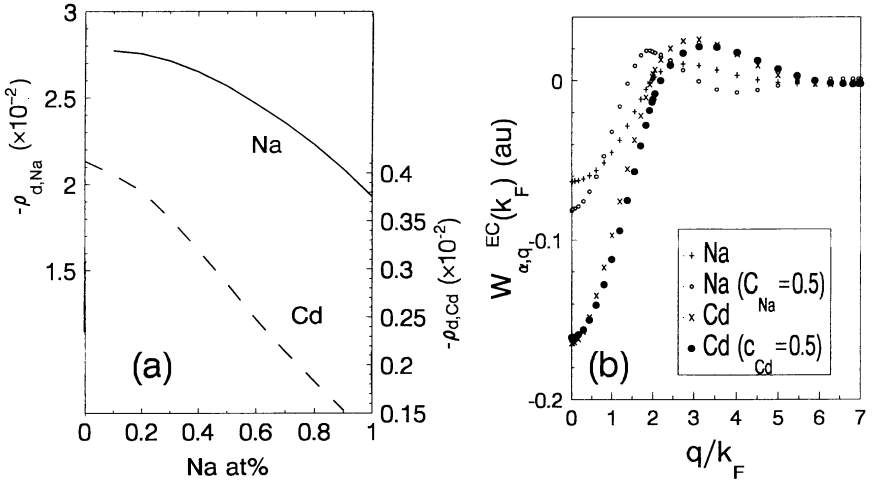

Figure 1. The depletion charges (a) and the on-Fermi-level form factors (b) calculated from EINMP theory for the ions in the liquid Na–Cd alloys.

2. Interatomic potentials

The interatomic potentials for binary alloys take the form

$$V_{\alpha\beta}(r) = Z_{\alpha,eff} Z_{\beta,eff} \left[1 - \frac{1}{\pi} \int_0^\infty (F_{\alpha\beta}(q) + F_{\beta\alpha}(q)) \frac{\sin qr}{q} \, \mathrm{d}q \right] \tag{1}$$

with $Z_{\alpha,eff}$ and $F_{\alpha\beta}(q)$ being respectively the effective valence for the α-type ions and the normalized energy–wavenumber characteristic, as defined in the EINMP theory. An assumption has been made that the bare ionic pseudopotential for each alloy constituent does

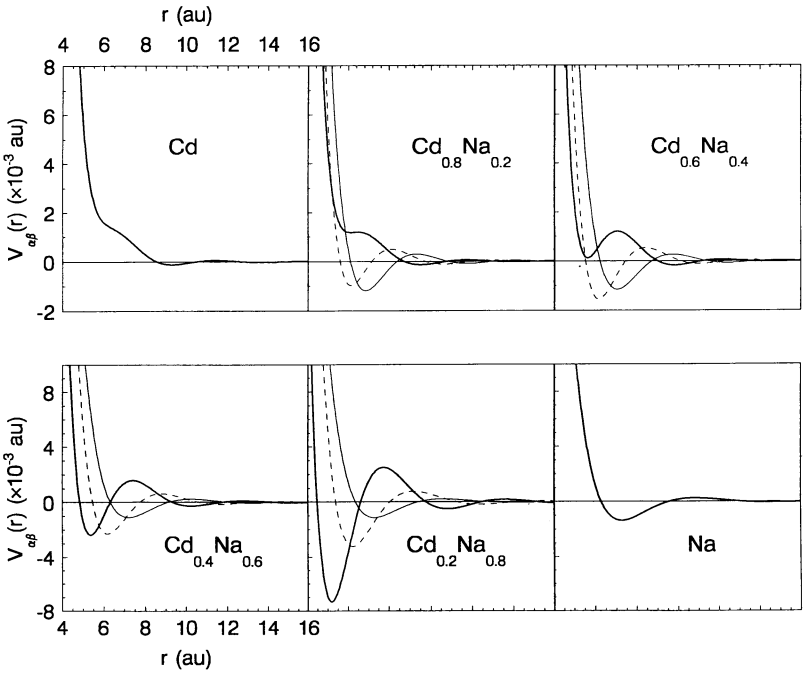

Figure 2. The interatomic potentials for the liquid Cd_cNa_{1-c} ($c = 1.0$, 0.8, 0.6, 0.4, 0.2 and 0) alloys at 673 K. Thick line: Cd–Cd; thin line: Na–Na; Dashed line: Cd–Na.

not change over the whole alloy concentration range. For alloys with weak and intermediate chemical interactions, such an assumption is acceptable. The concentration-dependent change in the interatomic pair potentials is mainly determined by the orthogonalization and the screening effects on the pseudopotentials. According to the discussion of Hafner (1987), the orthogonalization effect in alloys can be related to an electron transfer mechanism, i.e., the ion with lower electron density and hence an increase in orthogonalization hole charge (the depletion charge) transfers electrons to the ion with higher electron density, and so a decrease in the depletion charge occurs. For Na–Cd, such an effect can be expected when we examine the calculated depletion charges for both Na and Cd ions. As shown in figure 1(a), the depletion charge for Cd decreases and that for Na increases, which suggests that a charge transfer from Na to Cd should occur in Na–Cd alloys. This effect can be expected to be even more pronounced in the Cd-rich region, and leads to a stronger preference for chemical ordering. The screening effect describes the linear response of the conduction electron to the pseudopotential of the ion plus the orthogonalization hole. Of course, such a screening will be concentration dependent. This can be seen from the EINMP-calculated on-Fermi-level form factors for Na and Cd as in the case of $Na_{0.5}Cd_{0.5}$ shown in figure 1(b). It is found that, in comparing with that of the pure metal state, the change in the form factor for the electropositive component (Na) appears to be larger than that for the electronegative component (Cd). According to the argument of Wang and Lai (1980), such a change is reasonable for use in calculation of the pair potentials within the low-order pseudopotential theory, since the actual pseudopotential involved is weighted by the concentration of each component through its structure factors. The calculations will also depend on the choice of the exchange–correlation function. For the present Na–Cd alloy, we use the form of

Ichimaru and Utsumi, because in doing so (i) more accurate thermodynamic and structural results for pure metals can be obtained, especially for the polyvalent elements, and (ii) the chemical effects can be taken into account more accurately than in other forms used previously, e.g., by Wang and Lai (1980).

The calculated interatomic pair potentials for Na–Cd at 673 K with experimentally measured atomic volumes (Hoshino and Endo 1982) as input are shown in figure 2, for alloys at selected concentrations. For pure metal Cd, the peculiar potential curve (e.g., see the ledge at the nearest-neighbour position) is very similar to that for Zn (Moriarty 1983), which has been interpreted as being due to the filled 3d band in zinc, and accounts for the unusual high c/a ratio of the hcp phase for solid Zn or Cd metal. For alloys, the repulsive core of the effective-pair potentials is mainly influenced by the orthogonalization effect, while the form of the interatomic potentials around the nearest-neighbour distances is mainly influenced by screening effects. For Cd-rich alloys, the above two effects together yield a preferential interaction for unlike atoms which demonstrates a tendency toward chemical ordering. The reduced screening with decreasing electron density and the strong increase of the on-Fermi-level form factor for Cd on alloying with Na leads the Cd–Cd interactions in Na-rich alloys to be strongly attractive at short interaction distances. It should be noted that such changes are acceptable because the Cd–Cd interactions are just strong enough to induce the formation of Cd clusters, but not strong enough to drive the system into complete segregation in the Na-rich alloys. The systematic changes presented by the interatomic potentials on increasing the Na concentration are essential in both the thermodynamic and the structural calculations for the Na–Cd alloys, which exhibit quite interesting chemical effects.

3. Entropy of formation

In this section, we present a simple approach in the prediction of the mixing entropy for Na–Cd following the work of Hafner *et al* (1984). In their theory, by using a HSY reference system, the entropy of formation is decomposed into a hard-sphere contribution (taking account of number density fluctuations), an ordering contribution (accounting for concentration fluctuations) and a very small electronic contribution:

$$\Delta S = \Delta S_{HS} + \Delta S_{ord} + \Delta S_e \tag{2}$$

with ΔS_{HS} given by

$$\Delta S_{HS} = \Delta S_{id} + \Delta S_{gas} + \Delta S_\eta \tag{3}$$

where ΔS_{id} is the ideal mixing entropy, ΔS_{gas} is the ideal-gas contribution and ΔS_η is the hard-sphere packing contribution, with the exact forms being respectively written as

$$\Delta S_{id}/k_B = -(c_1 \ln c_1 + c_2 \ln c_2) \tag{4}$$

$$\Delta S_{gas}/k_B = \ln(\Omega_0/\Omega_1^{c_1}\Omega_2^{c_2}) \tag{5}$$

and

$$\Delta S_\eta = S_\eta - \sum_{i=1}^{2} c_i S_{\eta,i} \tag{6}$$

with $S_\eta/k_B = -\eta(4-3\eta)/(1-\eta)^2$ calculated using the Carnahan–Starling (1969) approximation. Here, η denotes the hard-sphere packing fraction for the alloy, η_i is that for the i-type unmixed constituent and c_i the concentration. The atomic volumes Ω_0 for the alloy and Ω_i for each element in the pure metal state can be taken from the experimentally

measured values (see, e.g., Hoshino and Endo 1982). The second term in equation (2) can be calculated from the following expression:

$$\Delta S_{ord}/k_B = [f(w) - f(0)]/2\eta \tag{7}$$

with the definition of $f(w)$ being given in detail by Hafner *et al* (1984) in an analytical solution for a system of hard spheres satisfying the 'charge-neutrality condition', with equal diameters σ and Yukawa tails within the mean-spherical approximation (MSA). For simplicity, we only note here that w is a function of three parameters at a given temperature, i.e., the hard-sphere diameter (σ), the strength of the ordering potential at contact (ε) and a screening constant (κ), which are combined to define a HSY-form ordering potential:

$$\phi_{cc}(r) = \begin{cases} \infty & r < \sigma \\ -\varepsilon\sigma \exp[-\kappa(r-\sigma)]/r & r \geqslant \sigma. \end{cases} \tag{8}$$

The analytic solution of the concentration and number fluctuation structure factors can also be given within such a model (see equation (30) of Hafner *et al* (1984) for details).

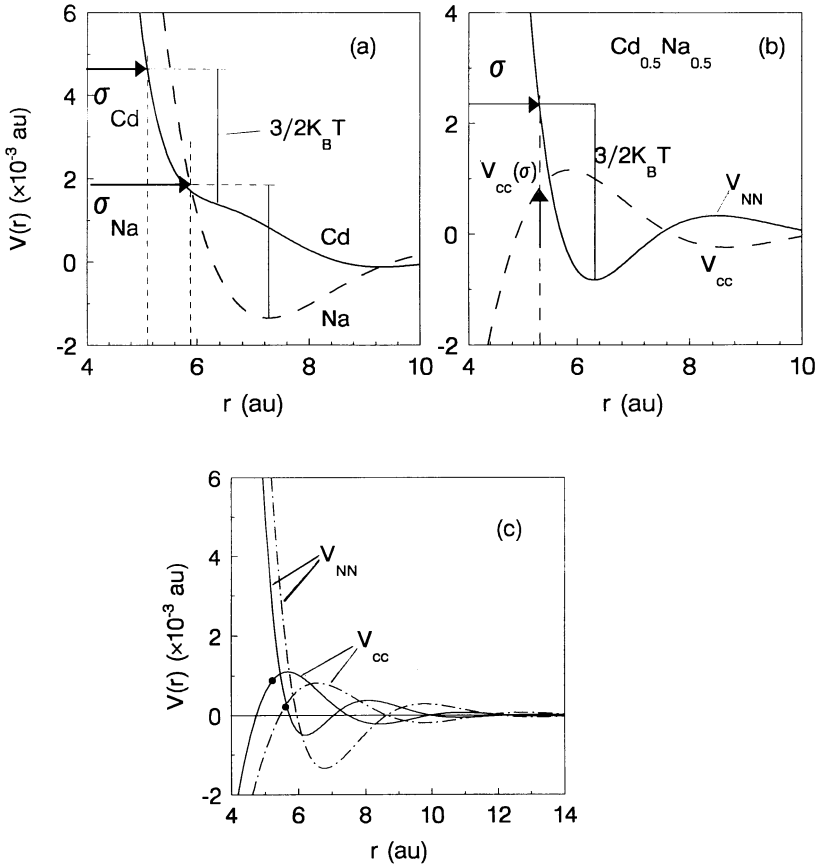

Figure 3. Hard-sphere diameter determinations using the simple relation (9) for (a) the pure Na and Cd metals and (b) $Na_{0.5}Cd_{0.5}$ alloy at 673 K. The mean and ordering potentials calculated according to equation (11) are presented in (c) for liquid $Na_{0.4}Cd_{0.6}$ (the full line) and $Na_{0.8}Cd_{0.2}$ (the chain line) alloys.

There are several possible ways to obtaining the HSY parameters ε, σ and κ: (i) from a first-principles thermodynamic variational method (Pasturel and Hafner 1985); and (ii) from experimental data (Hafner *et al* 1985). However, in our calculations, we use the following simple rule, which was first used by Ashcroft and Langreth (1967b) and was later further confirmed by Hafner (1977) and by Silbert and Young (1981), to determine the hard-sphere packing diameter σ:

$$V_{NN}(\sigma) = V_{NN}^{\min} + \frac{3}{2}k_B T \tag{9}$$

where $V_{NN}^{\min}$ is the depth of the first minimum in the mean interatomic potential $V_{NN}(r)$. Meanwhile, ε can be determined from the relation

$$\varepsilon = -\lambda V_{cc}(\sigma). \tag{10}$$

Here, V_{NN} and V_{cc} are the average and ordering potentials which are respectively defined as

$$\begin{aligned} V_{NN}(r) &= c_1^2 V_{11}(r) + c_2^2 V_{22}(r) + 2c_1 c_2 V_{12}(r) \\ V_{cc}(r) &= c_1 c_2 \left[V_{11}(r) + V_{22}(r) - 2V_{12}(r)\right]. \end{aligned} \tag{11}$$

Equation (10) was first suggested by Hafner *et al* (1984), but with the free parameter λ being set as unity. In our calculations, the λ-value has been determined by fitting the HSY-calculated concentration-dependent structure factor $S_{cc}(q)$ to the MD-calculated one at certain compositions of Na–Cd alloys (cf. figure 6, later). A mean value of 4.0 has been used in our present calculations. The remaining parameter κ is set as π/σ according to Hafner *et al* (1985). In particular, one point should be noted: in the determination of σ for pure Cd metal using the relation (9), σ corresponds to the repulsive part (the ledge) of $V(r)$ and not to the first minimum, as shown in figure 3(a). This is reasonable because in alloying with Na, this ledge will be deepened to bring out a minimum and the thus-determined value of η (0.442) is just the same as that used by Karaoglu and Young (1990) for pure Cd liquids. Figure 3(b) represents, as an example, the procedure of determination σ and $V_{cc}(\sigma)$ for the $Na_{0.5}Cd_{0.5}$ alloy. Also illustrated in figure 3(c) are the mean and the ordering potentials for two alloy cases in the CF and PS region. The relatively small ordering potential at the hard-sphere contact (denoted by a dot) for $Na_{0.8}Cd_{0.2}$ as compared to that of the $Na_{0.4}Cd_{0.6}$ alloy can qualitatively explain why the compound-forming tendency has been largely depressed in the Na-rich region.

Figure 4 displays our final results. The η–c_{Na} (figure 4(a)) and $V_{cc}(\sigma)$–c_{Na} (figure 4(b)) relationships both imply that the largest packing fraction and ordering potential locate on the Cd-rich side. The asymmetric ordering contribution to the excess entropy leads to a change in ΔS from negative to positive in value which corresponds to a CF-to-PS transition for this system. It is worth noting that the present HSY model does not cope with the contribution due to the phase separation explicitly, which may be related to the size factor for the system considered. Such a contribution should be important on the Na-rich side, and contribute positively to ΔS. However, it may be partially compensated by the slightly overestimated ΔS_{HS} which is due to a slightly underestimation of η for alloys in the Na-rich region in using equation (9), as compared with the results of Karaoglu and Young (1990). Despite some simplifications employed in the calculations, the agreement between the calculated and observed ΔS-value is satisfactory (cf. figure 4(c)). Since the conventional first-principles thermodynamics variation method based on the hard-sphere model which does not incorporate the ordering contribution to the free energies can hardly be used in a meaningful prediction of thermodynamic quantities like ΔS, it seems that our procedure used here for the calculation of the excess entropy for alloys exhibiting weak ordering effects

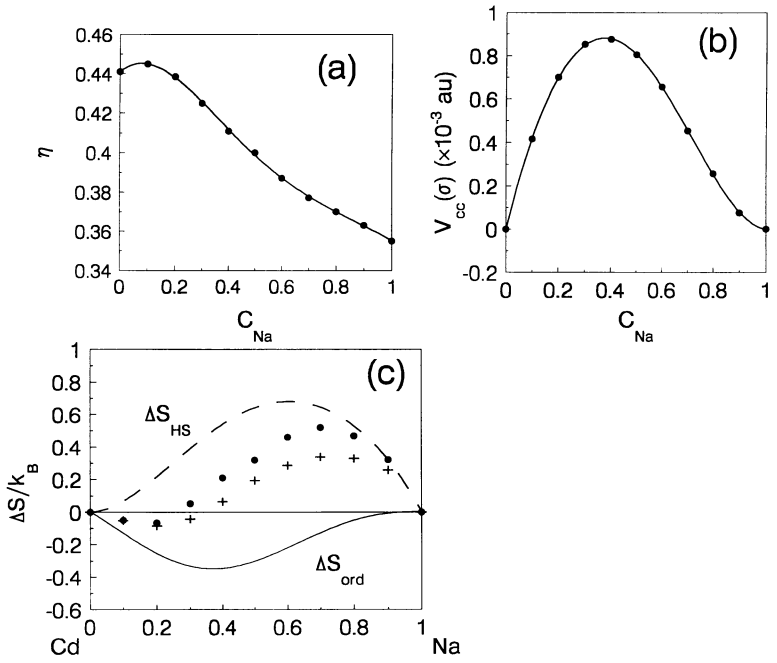

Figure 4. Na–Cd alloys at 673 K. (a) The packing fraction η, (b) the order potential at contact $V_{cc}(\sigma)$ and (c) the excess entropy ($\Delta S_{HS} + \Delta S_{ord}$) calculated using our present simple HSY model. The plus symbols denote the experimentally measured ΔS-value of Harada *et al* (1988).

is just as applicable as those—such as for some Li-based polyvalent alloys, demonstrated by Hafner *et al* (1985)—for which the ordering effects are relatively strong.

4. Topological and chemical short-range orders

The liquid structures of Na–Cd alloys at 673 K are simulated using molecular dynamics techniques. The MD procedure is carried out on a cubic box subjected to the widely used periodic boundary conditions with in total 1000 particles, via the effective-pair potentials calculated from equation (1). The potential is cut off at 21.0 au, and the time step is chosen as 5×10^{-15} s. In order to obtain an equilibrium liquid state, 12 000 sequential time steps have to be used. Twenty configurations are saved in another 4000 sequential time steps, one after each 200 time steps. Then, the steepest-descent energy minimization procedure with the conjugate method is imposed on each of these configurations to extract their inherent configurations, in which atoms are brought to a local minimum on the potential energy surface. Such an energy mapping method has been proved to be rather effective in establishing a unique structure–force relationship, independent of the thermodynamic parameters before mappings.

The structure analysis is divided into three parts. Firstly, the partial and total pair distribution functions ($g_{\alpha\beta}(r)$ and $g(r)$) and the structure factors (the Ashcroft–Langreth form and Bhatia–Thornton form) have been calculated and carefully examined. Secondly, the partial and total coordination numbers for each component in the alloy have been obtained and the Warren–Cowley-type chemical short-range-order parameter is calculated.

This parameter is a direct measure of the CSRO in both liquid and its inherent structures. And thirdly, we have used a pair analysis (PA) technique with the index of Honeycutt and Anderson (1987) to study the topological local order. The emphasis is placed mainly upon the changes of these properties with different alloy concentrations before and after mappings.

4.1. Distribution functions

The partial pair distribution functions $g_{\lambda\mu}(r)$ for a binary alloys are calculated from

$$g_{\lambda\mu}(r) = c_\mu \Omega_0 N_\lambda^{-1} \left\langle \sum_{i,j}{}' \delta(\boldsymbol{r} + \boldsymbol{R}_i^\lambda - \boldsymbol{R}_j^\mu) \right\rangle \tag{12}$$

where the $\boldsymbol{R}_i^\lambda$ $(i = 1, 2, \ldots, N_\lambda)$ are the positions of the λ-type atoms, and the sum is restricted to $i \neq j$ when $\lambda = \mu$. When disregarding the type of the atoms, equation (12) can yield the total pair distribution function $g(r)$. The Fourier transform of the $g_{\lambda\mu}(r)$ yields the partial structure factors of Ashcroft and Langreth (1967a) (hereafter A–L), i.e.,

$$a_{\lambda\mu}(q) = \delta_{\lambda\mu} + \frac{(c_\lambda c_\mu)^{1/2}}{\Omega_0} \int [g_{\lambda\mu}(r) - 1] \exp(\mathrm{i}\boldsymbol{q} \cdot \boldsymbol{r})\ \mathrm{d}\boldsymbol{r} \tag{13}$$

and from the A–L-type structure factor, the Bhatia–Thornton (B–T) type of structure factor can be calculated through a linear transformation:

$$\begin{aligned} S_{NN}(q) &= c_1 a_{11}(q) + 2(c_1 c_2)^{1/2} a_{12}(q) + c_2 a_{22}(q) \\ S_{Nc}(q) &= c_1 c_2 \left\{ a_{11}(q) + [(c_2/c_1)^{1/2} - (c_1/c_2)^{1/2}] a_{12}(q) - a_{22}(q) \right\} \\ S_{cc}q) &= c_1 c_2 [c_2 a_{11}(q) - 2(c_1 c_2)^{1/2} a_{12}(q) + c_1 a_{22}(q)]. \end{aligned} \tag{14}$$

For a detailed description of the calculations of distribution functions and the structure factors, one can refer to Waseda (1980) and Young (1992).

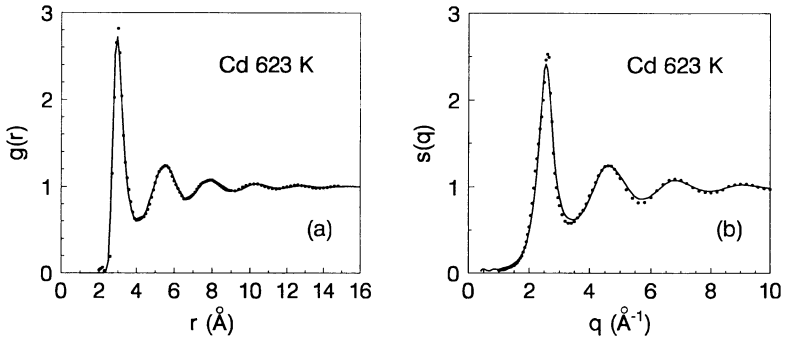

Figure 5. The MD-calculated pair distribution function $g(r)$ and structure factor $s(q)$ for liquid Cd metal at 623 K. The experimental data of Waseda (1980) are denoted by dots.

First, let us examine the $g(r)$ and $s(q)$ calculated for pure metal Cd, since Na has been well studied (Qi *et al* 1992). The results are shown in figure 5. An excellent agreement has been demonstrated on comparing the experimental diffraction data (Waseda 1980) for this metal at slightly above its melting points. The skew peak for $s(q)$ is also well known for Zn liquid, which is due to the peculiar ledge presented in the potential curves as shown in

figure 2. We shall assume that such a feature is related to the particular geometrical features characterized by 1311- and 1422-type local atomic units analysed in the subsection 4.3.

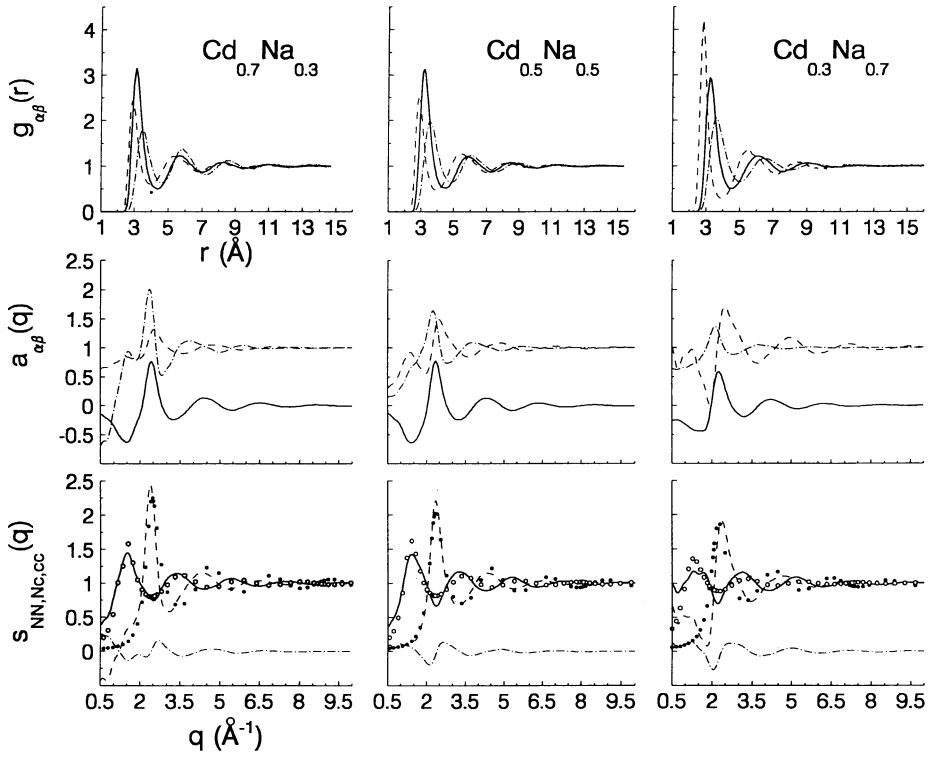

Figure 6. The pair distribution function $g_{\alpha\beta}(r)$, and the A–L-form and B–T-form structure factors ($a_{\alpha\beta}(q)$ and $S(q)$) calculated in the MD simulations for some Na–Cd alloys at 673 K. The B–T-form structure factors calculated using the HSY model are also illustrated by empty and full circles for comparison. Full line: Na–Cd or $S_{cc}(q)$; chain line: Na–Na or $S_{Nc}(q)$; dashed line: Cd–Cd or $S_{NN}(q)$.

Now we come to a detailed examination of the partial structural functions calculated for the alloys. Three alloys, i.e. $Cd_{0.7}Na_{0.3}$, $Cd_{0.5}Na_{0.5}$ and $Cd_{0.3}Na_{0.7}$ have been chosen, of which the $g_{\alpha\beta}(r)$, $a_{\alpha\beta}(q)$ and B–T forms $S_{NN}(q)$, $S_{Nc}(q)$ and $S_{cc}(q)$ are illustrated in figure 6. The following points have been clarified. (i) For the 30 and 50 at.% Na alloys, the first peak of $g_{NaCd}(r)$ is higher than that of both $g_{NaNa}(r)$ and $g_{CdCd}(r)$, which implies a preference for unlike coordination. Such a chemical effect can also be reflected by the small prepeak presented in the $a_{NaNa}(q)$- and $a_{CdCd}(q)$-curves. For the 70 at.% Na case, these features disappear, which suggests the absence of any ordering tendency. (ii) $S_{cc}(q)$ is a direct measure of CSRO. The $S_{cc}(q)$s for the 30 and 50 at.% Na alloys are comparable in magnitude and both larger than that of the 70 at.% Na case. This occurs because the CSRO should reach its maximum in magnitude in the concentration range of 20 to 40 at.% Na, as we have shown in the prediction of ΔS. However, above the concentration of 50 at.% Na, the CF tendency will be depressed by the PS tendency with increasing Na concentration. (iii) The skew peak of $S_{NN}(q)$ for high-Cd-concentration alloys is shortened and becomes more like that for the hard-sphere-type packing with increasing Na concentration. (iv) The

HSY-calculated $S_{NN}(q)$ and $S_{cc}(q)$ (with the fitted parameter $\lambda = 4.0$; see section 2 for details) can provide a generally good description of the structural characteristics for Na–Cd alloys.

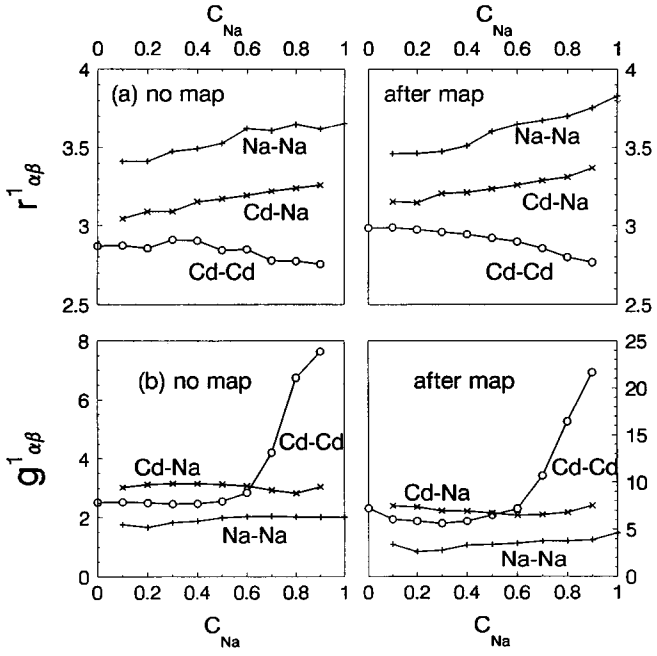

Figure 7. The position (a) and height (b) of the first peak of each of the partial pair distribution functions for the MD-simulated liquid Na–Cd alloys before and after potential energy mappings.

To make the above-noted points clearer, it is convenient to perform a further examination on the $g_{\alpha\beta}(r)$s for the alloys both before and after the potential energy mappings. Here, two parameters, i.e. the first peak position $r^1_{\alpha\beta}$ and the height of the first peak $g^1_{\alpha\beta}$ have been determined, and their concentration dependence has been illustrated in figure 7. The following features have been noted. From figure 7(a), we found that the Na–Na nearest-neighbour distance r^1_{NaNa} shrinks in going from the Na-rich region to the Cd-rich region, while r^1_{CdCd} changes slightly in the Cd-rich region and, above 50 at.% Na, decreases continuously with increasing Na concentration. The ratio of the shrinkage to the pure metal state of r^1_{NaNa} is about 7% for the $Na_{0.1}Cd_{0.9}$ case—larger than that of r^1_{CdCd} (about 3.5%) in $Na_{0.9}Cd_{0.1}$—which suggests that the volume contraction is largely determined by the chemical compression effects of Na. The enhanced difference between r^1_{NaNa} and r^1_{CdCd} with increasing Na concentration may directly account for the PS tendency for the Na-rich alloys. The mapping results, as shown in figure 7(b), demonstrate that all of the above-noted features have been maintained in the inherent structures and, to some extent, have been brought out as being more distinct. Following this, let us have a comparison of the height of the first peak shown in figure 7(c). It is found that g^1_{NaCd} appears to be the highest one up to 60 at.% of Na, both before and after mappings. This confirms our former remark on the CSRO for the alloy system—that the CSRO is characterized by the ordering effects in the Cd-rich region. Above 70 at.% of Na, g^1_{CdCd} is dramatically increased, especially after mappings, which implies a strong preference for the like pair of Cd–Cd. Such a

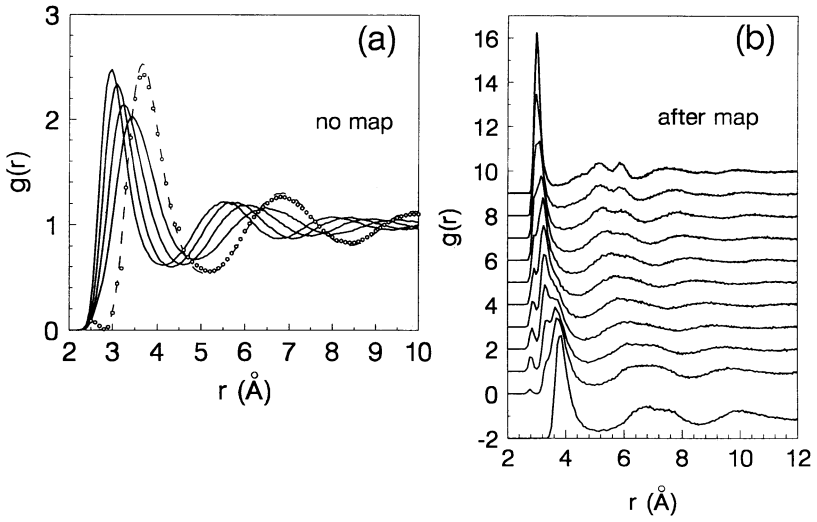

Figure 8. (a) The MD-calculated total pair distribution functions for Cd_cNa_{1-c} (with c being, from left to right, 0.8, 0.6, 0.4 and 0) liquid alloys at 673 K. The dashed line shows $g(r)$ for pure Na metal at 378 K and the dots denote the experimental data of Waseda (1980) for Na. (b) The total pair distribution functions calculated for the inherent structures of Cd_cNa_{1-c} (with c being, from top to bottom, 1.0, 0.9, 0.8, 0.7, 0.6, 0.5, 0.4, 0.3, 0.2, 0.1 and 0) alloys.

feature should be attributed to the strongly deepened minimum in the Cd–Cd interactions as shown in figure 2 for the Na-rich alloys. The above-presented concentration-dependent features in the changes of $r^1_{\alpha\beta}$ and $g^1_{\alpha\beta}$ can bring about a systematic change in the total pair distribution functions before and after mappings (cf. figure 8). Before mappings, the first main peak of the alloy has been deepened and widened by increasing Na concentration. After mappings, the complex profiles of the first main peak indicate that a systematic trend occurs in which there is a substantial division into three sub-maxima, which correspond to the Cd–Cd, Cd–Na and Na–Na distribution positions respectively, with the height (which should be concentration weighted) and the position being consistent with the above-noted $r^1_{\alpha\beta}$s and $g^1_{\alpha\beta}$s. It should be noted that all of these features, as well as the substantial changes in the second main peaks of the $g(r)$s, are initially correlated with the detailed local atomic orderings, which will be analysed in detail in the subsection 4.3. Before doing this, let us make a careful study of the CSRO parameter for the Na–Cd alloys in the following section.

4.2. CSRO

The CSRO can be obtained from knowledge of $S_{cc}(q)$ as shown in figure 6. However, a more quantitatively examination is possible on using the Warren–Cowley-type CSRO parameter defined as

$$\alpha^1 = 1 - \frac{Z_{AB}}{c_B Z} \tag{15}$$

where Z_{AB} is the number of B-type nearest neighbours of the A component, and Z is the total mean coordination number for an atom in the alloy. The parameter α^1 is known to represent the degree of preference for unlike- or like-atom neighbours. $0 < \alpha^1 < 1$ corresponds to a preference for like neighbours (PS or clustering); $\alpha^1 = 0$ to a statistically

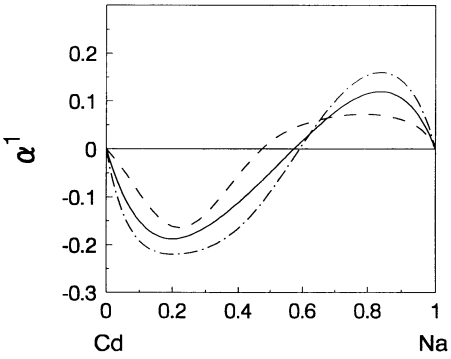

Figure 9. The chemical short-range-order parameter calculated for the liquid Na–Cd alloys at 673 K before (the full line) and after (the chain line) the potential energy mappings. The calculated results of Singh *et al* (1991) are denoted by the dashed line.

random distribution; and $\alpha^1 < 0$ to a distribution for unlike-atom-preference neighbours (a CF tendency or chemical ordering). The coordination number Z_{AB} can be easily counted by computer from the 20 MD saved configurations before and after mappings, with the nearest-neighbour distances being set as being the first minimum position of each $g_{\alpha\beta}(r)$. The calculated result for α^1 has been demonstrated in figure 9 for liquid Na–Cd before and after mappings, and shown to be in reasonable agreement with the calculated results of Singh *et al* (1991) based on the complex-formation model. The S-shape curve indicates that a strong chemical ordering should occur below the concentration of 40 at.% Na, the phase-separation tendency should be found above 60 at.% Na, and the CF-to-PS transition should take place in the concentration range of 50 to 60 at.% Na. Potential energy mapping does not change the CSRO tendency very much; to some extent, however, it leads to both an enhancement of the CF tendency on the Cd-rich side and an enhancement of the PS tendency on the Na-rich side.

4.3. TSRO

We use the pair analysis technique to study the topological short-range order in liquid Na–Cd. The PA method is based on the characterization of the various atomic bonded pairs. If two atoms are within a given cut-off separation, here chosen to be the position of the first minimum in the corresponding $g_{\alpha\beta}(r)$s, we say that the two atoms form a bond. Each atomic bonded pair can be characterized by four indices. As an example, the 1551 bonded pair represents the two root pair atoms with five common neighbours that form a pentagon of nearest-neighbour contacts, so the 1551 bond is situated in a fivefold-symmetry environment. And the number of 1551 bonds is a direct measurement of the degree of icosahedral ordering. The relative numbers of the various atomic bonded pairs which appear to be concentration sensitive for Na–Cd alloys have been illustrated in figure 10. Pure Cd metal is unique because, as mentioned in subsection 4.1, it shows a skew peak in $S(q)$ due to the particular potential curve around the nearest-neighbour distance. The PA result suggests that such a uniqueness can be characterized by the dominant appearance of a relatively large number (up to 17%) of 1311-type bonded pairs plus 16% 1431 and 12% 1422 pairs. The 1311- and 1422-type pairs are found to be related to a distorted hcp (high c/a ratio) structure according to our recent studies. For Na metal, it has been found that the 1551, 1541 and

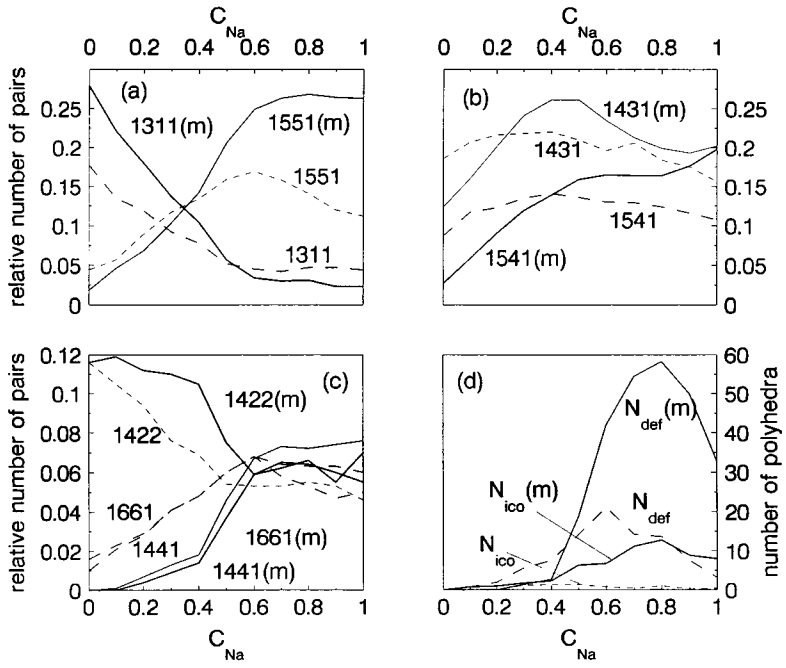

Figure 10. Pair analysis results for liquid Na–Cd alloys. The 'm' in parentheses denotes the results on the inherent structures obtained by potential energy mappings.

1431 pairs appear to be numerous. Since Na crystalline solids at room temperature exhibit bcc structure, some 1441 and 1661 pairs (dominating the bcc structure) also appear in its liquid state. So when Na and Cd are mixed together, we can expect a systematic change from a Cd-type liquid structure to a Na-type liquid structure. Such a change does indeed occur in the Na–Cd alloys, as shown in figure 10. The following points deserve to be noted. (i) The number of 1331-type bonded pairs decreases almost linearly as the concentration of Na increases to about 60 at.% both before and after mappings. However, the number of 1551 bonds first increases, reaches its maximum at 50 at.% Na, then above 70 at.% Na decreases slightly for the non-mapping case. After mappings, the number of 1551 bonds is almost constant above 70 at.% Na. (ii) The above-noted concentration-dependent features for 1331 and 1551 bonds are accompanied by changes in the features of 1431 and 1541 bonds. As shown in figure 10(b), before mappings, the number of 1431 bonds first increases slightly, then above 40 at.% Na it decreases. After mappings, the number of 1431 bonds reaches its maximum dramatically at about 40 at.% Na, then decreases until 90 at.% Na is reached. (iii) The changes in the number of 1422, 1661 and 1441 bonds are very similar to the changes in numbers of 1311 and 1551 bonds as shown in figure 10(c), which also suggests that a particular concentration (60 at.% Na) exists after which the particular local atomic ordering units such as 1311- and 1422-type bonds have been largely depressed and replaced by the overwhelming appearance of 1511, 1541, 1661 and 1441 bonds. Hence, we postulate that this happens because the chemical effects should also play an important role in the fine local atomic orderings for the Na–Cd alloy. (iv) Since each icosahedron is formed by twelve 1551 bonded pairs, the number (N_{ico}) of icosahedra is directly influenced by the number of 1551 pairs. However, although the number of 1551 atomic pairs is large

before mappings, N_{ico} appears to be very small. Only after mapping does N_{ico} appear to be comparable with the number of defective polyhedra. The number of defective polyhedra is the sum of the total number of defective icosahedra, Bernal hole polyhedra and Frank–Kasper polyhedra (see Qi and Wang 1991). For Na–Cd, above 40 at.% Na, N_{def} appears dominant, especially after mappings—it is almost six times larger than N_{ico}.

Our results demonstrate that TSRO can be identified rather effectively, via the PA formula, in that the local atomic order changes systematically on going from Cd-rich alloys characterized by the 1311- and 1422-type bonds to the 1551-type structure for the Na-rich alloys. However, the changes in the numbers of the various atomic bonded pairs and polyhedra are not in a simple linear relation to the alloy concentration, since the chemical effects also have an important influence. Hence, similarly to CSRO, TSRO also exhibits a transition in the concentration range of 50 to 60 at.% Na.

5. Conclusion

We have performed a systematic investigation of both the chemical and topological short-range order for liquid Na–Cd alloys, using EINMP-derived interatomic potentials. We conclude as follows.

(i) The entropy of formation can be predicted in good agreement with the experimental data, in the framework of a HSY model whose parameters are determined from the mean interactions and the ordering potentials.

(ii) MD simulations combined with a potential energy mapping technique have been used in the calculations of the structural functions, and chemical short-range-order parameters. We found that the ordering effects are relatively strong on the Cd-rich side. When the Na concentration is increased, a tendency towards phase separation has been observed, which is substantially influenced by the clustering effect of the Cd component. This observation has been confirmed via the calculation of the chemical short-range-order parameters. It seems that the mapping procedure does not change the chemical ordering tendency very much; however, there is an enhancement of the chemical effects on both the compound-formation side and the phase-separation side for the Na–Cd after mappings.

(iii) The pair analysis results demonstrate that the topological short-range order in Na–Cd changes from a Cd-type structure characterized by 1311- and 1422-type atomic bonds to a Na-type structure dominated by 1551-type atomic bonded pairs, systematically. A characteristic composition (about 60 at.% Na) exists for such a change, which should be attributed to the chemical effects. The potential energy mappings can bring out the physical picture of the local atomic orderings even more clearly.

References

Ashcroft N W and Langreth D C 1967a *Phys. Rev.* **156** 685 (erratum: 1968 **166** 934)
——1967b *Phys. Rev.* **159** 500
Carnahan N F and Starling K E 1969 *J. Chem. Phys.* **51** 635
Hafner J 1977 *Liquid Metals 1976 (Inst. Phys. Conf. Ser. 30)* (Bristol: Institute of Physics Publishing) p 102
——1987 *From Hamiltonians to Phase Diagrams* (Berlin: Springer)
Hafner J, Pasturel A and Hicter P 1984 *J. Phys. F: Met. Phys.* **14** 1137
——1985 *Z. Metallk.* **76** 432
Harada S, Takahashi S, Takeda S, Tamaki S, Gray P and Cusack N E 1988 *J. Phys. F: Met. Phys.* **18** 2559
Honeycutt H R and Andersen H C 1987 *J. Chem. Phys.* **91** 4950
Hoshino H and Endo H 1982 *Phys. Chem. Liq.* **11** 327
Ichimaru S and Utsumi K 1981 *Phys. Rev.* B **24** 7285

Iwase M, Sugino S, Ichise E and Waseda Y 1985 *J. Chem. Thermodyn.* **17** 601
Karaoglu B and Young W H 1990 *J. Phys. C: Solid State Phys.* **2** 9189
Li D H, Li X R and Wang S 1986 *J. Phys. F: Met. Phys.* **18** 307
Moriarty J A 1983 *Int. J. Quantum Phys.* **17** 541
Pasturel A and Hafner J 1985 *Phys. Rev.* B **32** 5009
Qi D W, Lu J and Wang S 1992 *J. Chem. Phys.* **96** 513
Qi D W and Wang S 1991 *Phys. Rev.* B **44** 884
Ruppersberg H and Speicher W 1976 *Z. Naturf.* a **31** 47
Silbert M and Young W H 1981 *J. Phys. C: Solid State Phys.* **14** 2425
Singh R N, Jha I S and Sinha S K 1991 *J. Phys.: Condens. Matter* **3** 2787
Stillinger F H and Weber T A 1982 *Phys. Rev.* A **25** 978
Tamaki S and Cusack N E 1979 *J. Phys. F: Met. Phys.* **9** 403
Tsay S F and Wang S 1994 *Phys. Rev.* B **50** 108
Wang S and Lai S K 1980 *J. Phys. F: Met. Phys.* **10** 2717
Waseda Y 1980 *The Structure of Non-Crystalline Materials* (New York: McGraw-Hill)
Young W H 1992 *Rep. Prog. Phys.* **55** 1769